ARTICLE IN PRESS

JOURNAL OF BIOMECHANICS

Journal of Biomechanics ▮ (▮▮▮▮) ▮▮▮–▮▮▮

www.elsevier.com/locate/jbiomech
www.JBiomech.com

Short communication

Artificial composite bone as a model of human trabecular bone: The implant–bone interface

J.A. Grant[a], N.E. Bishop[a], N. Götzen[a], C. Sprecher[b], M. Honl[c], M.M. Morlock[a,*]

[a]Biomechanics Section, TUHH Hamburg University of Technology, Denickestrasse 15, Hamburg D-21073, Germany
[b]AO Research Institute, Davos, Switzerland
[c]Rush University Medical Centre, Chicago, USA

Accepted 14 April 2006

Abstract

The use of artificial bones in implant testing has become popular due to their low variability and ready availability. However, friction coefficients, which are critical to load transfer in uncemented implants, have rarely been compared between human and artificial bone, particularly for wet and dry conditions. In this study, the static and dynamic friction coefficients for four commercially used titanium surfaces (polished, Al_2O_3 blasted, plasma sprayed, beaded) acting on the trabecular component of artificial bones (Sawbones®) were compared to those for human trabecular bone. Artificial bones were tested in dry and wet conditions and normal interface stress was varied (0.25, 0.5, 1.0 MPa). Friction coefficients were mostly lower for artificial bones than real bone. In particular, static friction coefficients for the dry polished surface were 20% of those for real bone and 42–61% for the dry beaded surface, with statistical significance ($\alpha < 0.05$). Less marked differences were observed for dynamic friction coefficients. Significant but non-systematic effects of normal stress or wet/dry condition on friction coefficients were observed within each surface type. These results indicate that the use of artificial bone models for pre-clinical implant testing that rely on interface load transfer with trabecular bone for mechanical integrity can be particularly sensitive to surface finish and lubrication conditions.

Keywords: Friction; Bone–implant interface; Artificial bone; Pre-clinical testing; Press fit

1. Introduction

Artificial bones are regularly used in pre-clinical testing of implants (Harman et al., 1995; McKellop et al., 1991; Monti et al., 1999; Otani et al., 1993; Viceconti et al., 2001). For implants that rely primarily on press-fit for stability, the friction conditions play a major role in interfacial load transfer (Orlik et al., 2003; Rubin et al., 1993). In many modern proximally anchored femoral stems, the stem interfaces predominantly with the trabecular bone component. The purpose of this study was therefore to measure the friction coefficients of artificial trabecular bone acting under both dry and wet conditions and to compare them with those for human trabecular bone, using a range of commercial implant surface finishes and varying normal load.

2. Materials and methods

The artificial bones tested in this study were ‘third generation’ femoral Sawbones® (Product code 3303, Pacific Research Laboratories, WA, USA).

2.1. Preparation of specimens

Four commercial titanium implant surfaces were tested, with a range of surface roughness (Fig. 1, Table 1). All implant surface samples were 30 mm diameter discs, designed to overlap the smaller bone specimens, to

*Corresponding author. Tel.: +49 40 42878 3253; fax: +49 40 42878 2996.
E-mail address: morlock@tuhh.de (M.M. Morlock).
URL: http://www.tu-harburg.de/bim/.

0021-9290/$ - see front matter
doi:10.1016/j.jbiomech.2006.04.007

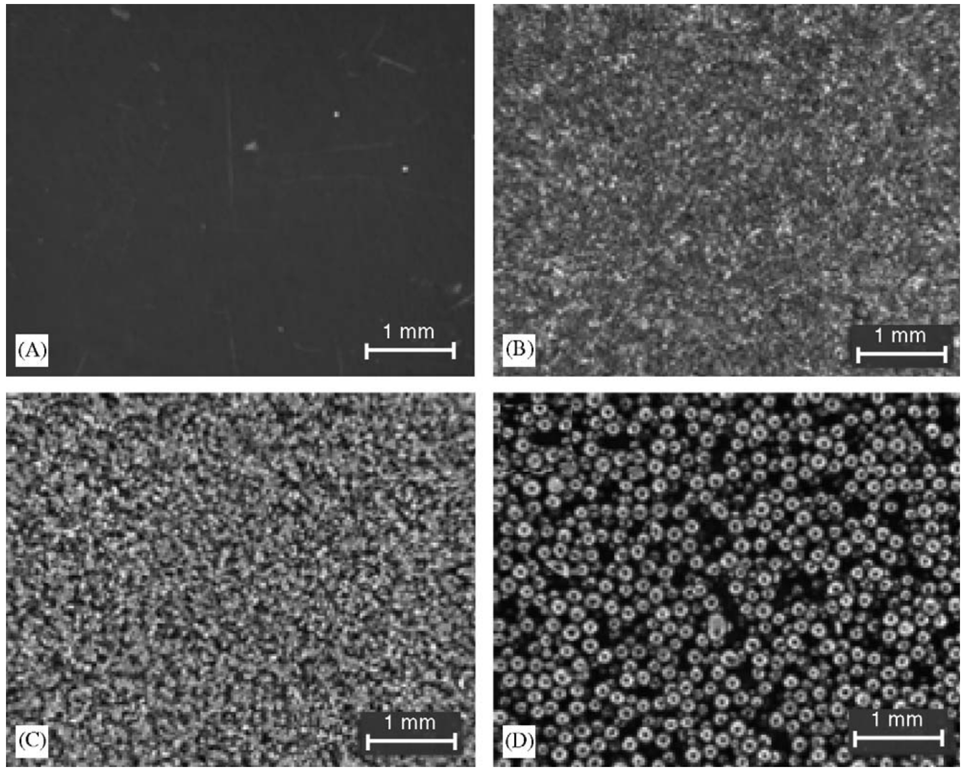

Fig. 1. Light microscope images of the four titanium surfaces: polished (A); Al_2O_3-blasted (B); plasma-sprayed (C); beaded (D). See Table 1 for R_a values.

Table 1
Surfaces used in the study in ascending order of roughness (R_a), measured with a Perthometer S6P laser profilometer (Feinpruf GmbH, Germany)

Implant surface	Manufacturer	R_a (μm)
Polished titanium	Aesculap, Germany	0.11
Al_2O_3-blasted titanium	Aesculap, Germany	11.00
Plasma-sprayed titanium	Aesculap, Germany	19.00
Beaded porous titanium	DePuy, UK	32.60

prevent edge effects. Three material conditions were compared: trabecular sawbone® in 20% fetal bovine serum (SB-Wet); trabecular sawbone® under dry conditions (SB-Dry); and human trabecular bone in 20% fetal bovine serum (HB). Human trabecular bone cubes were obtained from 7 cadaveric femora (Donor age: 56–72 years; density: 250–420 mg/cm^3). The bones were stored frozen at $-25\,^{\circ}$C. The frozen femora were transected distally below the articular surface in the transverse plane using a diamond-coated band saw blade (EXAKT Technologies Inc., OK, USA). Parallel bone cross sections with a thickness of 8 mm were harvested until the diaphysis was reached (average of 8 cross sections per distal femor). Rectangular bone cubes were cut from the sections ($14 \times 14 \times 8$ mm). Trabecular Sawbones® samples (polyurethane foam) of equivalent size were cut from Sawbone® femora. The human trabecular bone specimens were thawed at room temperature for approximately 1 h before testing and were assigned randomly to the different testing conditions.

2.2. Test apparatus

A 6 station, oscillating testing apparatus was used, based on ASTM 732-82 (Pin-on-flat), but inverted so that the softer material (flat) is displaced over the harder material (pin) (Fig. 2). The implant surface samples were inserted into the clamping collar on the lever–arm beam of each station (Fig. 3A). To ensure a good contact interface between the implant and the bone surfaces, the bone sample (Fig. 3B) was temporarily bound to the implant surface with a cotton thread. The specimen holder was then filled with methylmethacrylate (MMA) (Technovit 9100, HBS Sciences, CN, USA) and the bone specimen, attached to the implant surface by a cotton thread, was lowered into the holder, leaving about 2 mm above the cement surface. The MMA was left to polymerise around the bone specimen in the specimen holder for approximately 30 min.

Once the MMA had cured, the cotton thread holding the bone to the surface was removed. The wet sawbones and human bone groups were immersed in 20% foetal bovine serum (Kraeber GmbH & Co, Ellerbek, Germany) at 37 °C and allowed to equilibrate for 10 min.

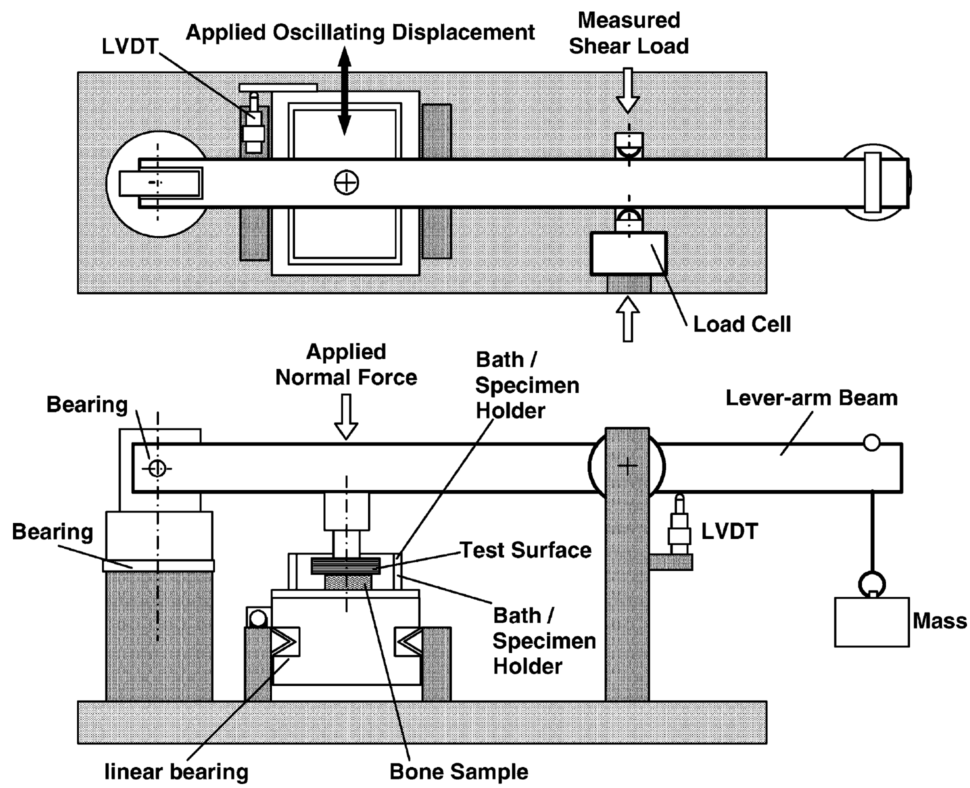

Fig. 2. Top and side views of the experimental test apparatus.

The implant surface was then placed in contact with the bone sample and a mass was applied to the end of the lever arm to create a normal force on the specimen. The specimen carriage, to which the sample holder was attached, was driven by a crank connected to a continuously rotating motor drive. The horizontal displacement of the carriage was measured using a linear variable displacement transducer (LVDT) (Penny & Giles, UK). The resulting lateral friction force between the specimen and bone was measured by the horizontal rotation of the lever–arm beam against a ± 2000 N tension-compression force transducer (Burster Präzisionsmeßtechnik GmbH, Germany) and scaled according to the moment arm lengths. The accuracy of the measurement system was ± 0.05 mm and ± 1 N. LVDTs and force transducers were digitally sampled at 150 Hz by SPIDER8 multi-channel digital acquisition hardware and processed by CATman data acquisition software (HBM, Inc., MA, USA).

2.3. Experimental procedure

The independent variables considered were: Type of implant surface used (4 types, Fig. 1 and Table 1); material condition (3 types: HB, SB-Wet, SB-Dry); magnitude of normal contact pressure (0.25, 0.5, 1.0 MPa). The normal load magnitudes were chosen to overlap with those used in other studies (Shirazi-Adl et al., 1993). A minimum of 5 bone samples were tested for each permutation of implant surface, bone type and normal load. The sliding carriage oscillated sinusoidally for 50 cycles with an amplitude of 1.1 mm and a frequency of 0.58 Hz.

The dependent variables were the static and dynamic friction coefficients. The static friction coefficient was determined by dividing the peak shear force (Fig. 4) by the normal force. The dynamic friction coefficient was calculated as the average shear force (Fig. 4) recorded over the velocity range of 80–100% of the maximum carriage velocity ($\approx$4 mm/s) divided by the normal force. The mean value for the 30th–50th displacement cycles was used for analysis, in an attempt to represent the steady-state interface conditions once the implant has ‘bedded-in’.

Three-way analysis of variance was performed with load, surface and bone type as factors. Tukey-B post hoc comparisons made and presented if interactions between the factors were found to be significant ($\alpha = 0.05$).

3. Results

3.1. Static friction

All observed differences in combined (averaged for contact pressure and material condition) static friction

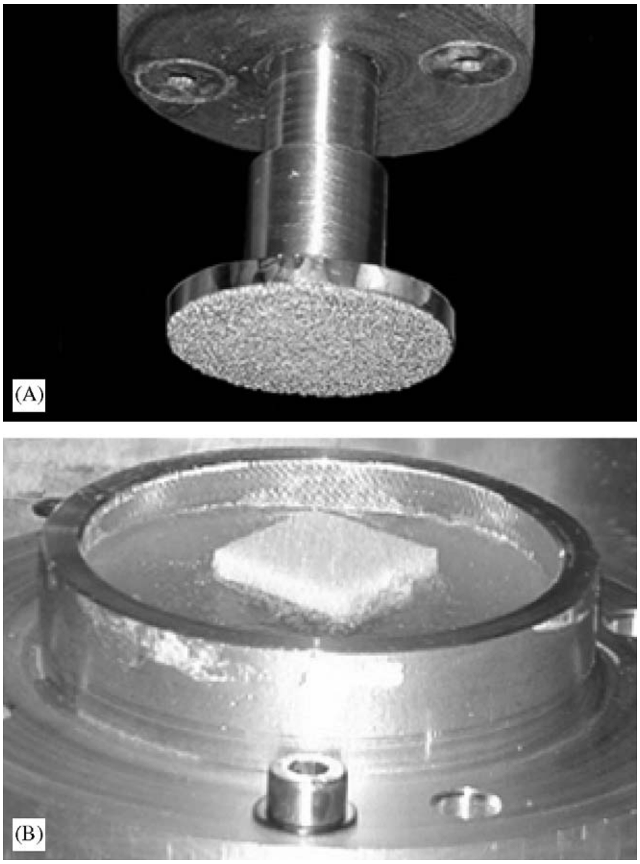

Fig. 3. Example for the two interface surfaces: titanium surface on 30 mm disc (A); 14 × 14 × 8 mm bone specimen embedded in cement (B).

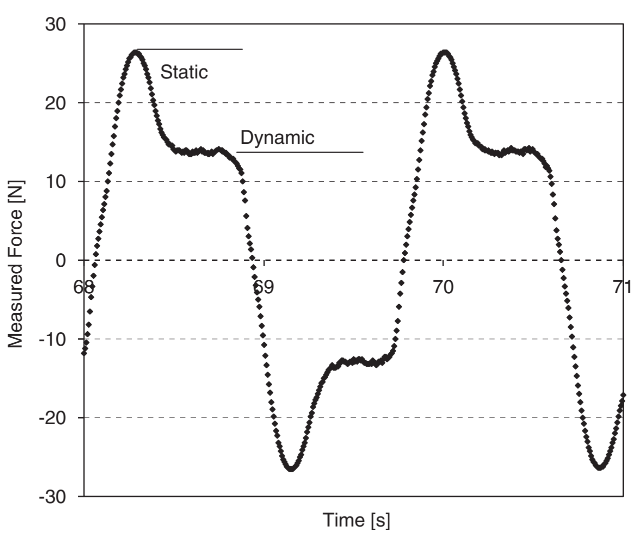

Fig. 4. Typical example of the raw data, showing well-defined peaks (static friction) and plateaus (dynamic friction).

values between the four implant surfaces were significant, with lowest values for the polished surface and greatest for the Plasma-sprayed surface ($p<0.001$; Table 2). Combined (averaged for contact pressure and implant surfaces) static friction coefficients for dry Sawbones® were significantly lower than those for wet Sawbones® and both were significantly lower than human bone (SB-dry: 0.52 ± 0.25, SB-wet: 0.61 ± 0.17, HB: 0.77 ± 0.27; $p<0.001$). Similar results were observed between artificial and real bone for the polished surface on wet sawbones and for two load levels of the Al_2O_3-blasted surface on dry and wet sawbones (Table 2). The greatest differences observed in static friction coefficients were for the polished surface which on dry artificial bone were 20% of those for real bone ($p<0.001$), and for the beaded porous surface which on dry artificial bone were 30–40% of those for real bone ($p<0.001$). Coefficients for the beaded surface in wet artificial bone conditions were 63–73% of those for real bone ($p<0.001$). Strong interactions between normal load and implant surface were observed for all 4 surfaces ($p<0.001$ for SB-dry and SB-wet, $p = 0.004$ for HB), indicating a non-systematic influence of load increase on the static friction coefficient for the different implant surfaces.

3.2. Dynamic friction

The range of dynamic coefficient values observed for the textured surfaces was lower than for the static friction values, ranging from 0.22 to 0.58 (Table 3) compared to 0.43–1.24 for the static coefficients (Table 2). Among bone types, significant differences for dynamic coefficients were observed for the SB-dry condition, which exhibited the lowest values of any bone conditions (SB-dry: 0.36 ± 0.18, SB-wet: 0.44 ± 0.09, HB: 0.43 ± 0.12; $p<0.001$). SB-wet and HB showed no differences. The Al_2O_3-blasted and plasma-sprayed surfaces exhibited the highest dynamic friction coefficients and the polished surface the lowest ($p<0.001$, Table 3). Load level showed no influence in the combined analysis. Within each surface condition, however, differences were found: for the polished and the beaded porous surfaces, SB-dry exhibited significantly lower values than HB and SB-wet at all 3 normal loads ($p<0.001$ at all load levels). The plasma-sprayed and Al_2O_3-blasted surfaces showed less systematic results (Table 3).

4. Discussion

The friction coefficients acquired in this study represent a full matrix of a realistic range of surface types and normal loads for human trabecular bone and Sawbones®. Friction coefficients with human bone were very similar to magnitudes measured in other similar studies, for example, 0.39–0.44 for a smooth surface (Shirazi-Adl et al., 1993). However, lower coefficients than those found in this study were reported for beaded

Table 2
Static friction coefficients (mean ± SD)

Surface	Normal load (Mpa)	Bone type	*N*	Mean	SD	Sign. groups	*P*
Polished	0.25	SB-dry	6	0.08	0.01	a,b	< 0.001
		SB-wet	5	0.42	0.05		
		HB	13	0.41	0.04		
	0.50	SB-dry	6	0.08	0.01	a,b	< 0.001
		SB-wet	5	0.40	0.04		
		HB	5	0.40	0.03		
	1.00	SB-dry	6	0.08	0.01	a,b	< 0.001
		SB-wet	5	0.39	0.05		
		HB	13	0.39	0.04		
	Combined	Combined	64	0.31	0.15	X	< 0.001
Al_2O_3 Blasted	0.25	SB-dry	22	0.54	0.10	a	< 0.001
		SB-wet	9	0.55	0.08	c	
		HB	17	0.75	0.13		
	0.50	SB-dry	12	0.55	0.06	a,b	0.007
		SB-wet	9	0.70	0.09		
		HB	9	0.65	0.13		
	1.00	SB-dry	6	0.71	0.10	b	< 0.001
		SB-wet	9	0.56	0.06		
		HB	17	0.65	0.11		
	Combined	Combined	110	0.63	0.13	XX	
Plasma sprayed	0.25	SB-dry	5	0.66	0.08	a	< 0.001
		SB-wet	5	0.75	0.11	c	
		HB	4	1.24	0.19		
	0.50	SB-dry	9	0.97	0.15		0.318
		SB-wet	8	0.97	0.16		
		HB	13	1.07	0.19		
	1.00	SB-dry	10	0.60	0.09	a	< 0.003
		SB-wet	5	0.63	0.09	c	
		HB	5	0.80	0.11		
	Combined	Combined	64	0,87	0.24	XXX	
Beaded porous	0.25	SB-dry	14	0.43	0.07	a,b	< 0.001
		SB-wet	8	0.63	0.10	c	
		HB	18	1.00	0.15		
	0.50	SB-dry	5	0.53	0.04	a	< 0.001
		SB-wet	10	0.66	0.09	c	
		HB	19	0.96	0.19		
	1.00	SB-dry	9	0.50	0.04	a	< 0.001
		SB-wet	10	0.60	0.12	c	
		HB	19	0.82	0.14		
	Combined	Combined	112	0,74	0.24	XXXX	

Significant differences within each surface type and normal load are indicated: [a]significant differences between SB-D and HB, [b]significant differences between SB-D and SB-W, [c]significant differences between SB-W and HB.
Significant differences between surface types are indicated by the symbols X, XX, XXX and XXXX.

surfaces (0.50–0.62), which may be due to a lack of lubricant in their study.

The very low coefficients observed for dry Sawbones® may be due to a lubricating layer of fine particulate dust, which was observed on these surfaces. This powder layer, in combination with a polished surface or beaded surface (consisting of polished beads), could cause the lower coefficients. It remains to be seen whether such a layer would be generated in a whole-bone experiment. Friction coefficients for blasted and plasma surfaces were much less dependent upon wet or dry conditions, which could be due to the interdigitation arising from a sharper surface profile and asperities which penetrate through the lubricating layer.

These results are particularly relevant to the experimental testing of implants, which derive their mechanical integrity from press fitting into trabecular bone. Friction coefficients influence the mechanical stability of

Table 3
Dynamic friction coefficients (mean ± SD)

Surface	Normal load (Mpa)	Bone type	N	Mean	SD	Sign.	P
Polished	0.25	SB-dry	6	0.07	0.02	a	<0.001
		SB-wet	5	0.4	0.04		
		HB	13	0.38	0.04		
	0.50	SB-dry	6	0.07	0.01	a	<0.001
		SB-wet	5	0.39	0.04		
		HB	5	0.38	0.03		
	1.00	SB-dry	6	0.08	0.01	a	<0.001
		SB-wet	5	0.38	0.04		
		HB	13	0.35	0.04		
	Combined	Combined	64	0.29	0.14	X	
Al_2O_3 blasted	0.25	SB-dry	22	0.44	0.08	a,b	<0.001
		SB-wet	9	0.43	0.06		
		HB	17	0.54	0.10		
	0.50	SB-dry	12	0.58	0.07	a,c	0.007
		SB-wet	9	0.46	0.06		
		HB	9	0.45	0.14		
	1.00	SB-dry	6	0.53	0.08		
		SB-wet	9	0.48	0.06		
		HB	17	0.44	0.14		
	Combined	Combined	110	0.48	0.11	XXX	
Plasma sprayed	0.25	SB-dry	5	0.51	0.08		
		SB-wet	5	0.56	0.10		
		HB	4	0.48	0.12		
	0.50	SB-dry	10	0.47	0.10		
		SB-wet	9	0.45	0.13		
		HB	13	0.44	0.13		
	1.00	SB-dry	10	0.43	0.04	b,c	0.02
		SB-wet	5	0.53	0.09		
		HB	5	0.43	0.07		
	Combined	Combined	64	0.47	0.10	XXX	
Beaded porous	0.25	SB-dry	14	0.22	0.04	a	<0.001
		SB-wet	8	0.36	0.09		
		HB	18	0.42	0.13		
	0.50	SB-dry	5	0.27	0.02	a	0.007
		SB-wet	10	0.45	0.05		
		HB	19	0.42	0.12		
	1.00	SB-dry	9	0.3	0.05	a	0.034
		SB-wet	10	0.37	0.07		
		HB		0.41	0.13		
	Combined	Combined	112	0.37	0.12	XX	

Significant differences within each surface type and normal load are indicated: [a]significant differences between SB-D and HB, [b]significant differences between SB-W and HB, [c]significant differences between SB-D and SB-W.
Significant differences between surface types are indicated by the symbols X, XX, XXX and XXXX.

an implant, its relative motion in the bone, and affect reaming and seating of the implant in the bone. Consequently, bone substitute materials should mimic realistic friction conditions. This was not observed for many combinations of surfaces and contact loads, especially in the dry situation. The results of pre-clinical testing of uncemented implants with artificial bone substitutes should therefore be treated with caution. It is suggested that wetted artificial bones are used, to minimise the difference in friction coefficients.

Acknowledgment

Aesculap and DePuy for materials and Fullbright for J. Grant's scholarship.

References

Harman, M.K., Toni, A., Cristofolini, L., Viceconti, M., 1995. Initial stability of uncemented hip stems: an in-vitro protocol to measure torsional interface motion. Medical Engineering & Physics 17, 163–171.

McKellop, H., Ebramzadeh, E., Niederer, P.G., Sarmiento, A., 1991. Comparison of the stability of press-fit hip prosthesis femoral stems using a synthetic model femur. Journal of Orthopaedic Research 9, 297–305.

Monti, L., Cristofolini, L., Viceconti, M., 1999. Methods for quantitative analysis of the primary stability in uncemented hip prostheses. Artificial Organs 23, 851–859.

Orlik, J., Zhurov, A., Middleton, J., 2003. On the secondary stability of coated cementless hip replacement: parameters that affected interface strength. Medical Engineering & Physics 25, 825–831.

Otani, T., Whiteside, L.A., White, S.E., McCarthy, D.S., 1993. Effects of femoral component material properties on cementless fixation in total hip arthroplasty. A comparison study between carbon composite, titanium alloy, and stainless steel. Journal of Arthroplasty 8, 67–74.

Rubin, P.J., Rakotomanana, R.L., Leyvraz, P.F., Zysset, P.K., Curnier, A., Heegaard, J.H., 1993. Frictional interface micromotions and anisotropic stress distribution in a femoral total hip component. Journal of Biomechanics 26, 725–739.

Shirazi-Adl, A., Dammak, M., Paiement, G., 1993. Experimental determination of friction characteristics at the trabecular bone/porous-coated metal interface in cementless implants. Journal of Biomedical Materials Research 27, 167–175.

Viceconti, M., Cristofolini, L., Baleani, M., Toni, A., 2001. Pre-clinical validation of a new partially cemented femoral prosthesis by synergetic use of numerical and experimental methods. Journal of Biomechanics 34, 723–731.